JACS
JOURNAL OF THE AMERICAN CHEMICAL SOCIETY
Article
pubs.acs.org/JACS

Stable 3,6-Linked Fluorenyl Radical Oligomers with Intramolecular Antiferromagnetic Coupling and Polyradical Characters

Xuefeng Lu,[†] Sangsu Lee,[‡] Jun Oh Kim,[‡] Tullimilli Y. Gopalakrishna,[†] Hoa Phan,[†] Tun Seng Herng,[§] Zhenglong Lim,[†] Zebing Zeng,[∥] Jun Ding,[§] Dongho Kim,*[,‡] and Jishan Wu*[,†]

[†]Department of Chemistry, National University of Singapore, 3 Science Drive 3, 117543, Singapore

[‡]Spectroscopy Laboratory for Functional π-Electronic Systems and Department of Chemistry, Yonsei University, Seoul 120-749, Korea

[§]Department of Materials Science & Engineering, National University of Singapore, 119260, Singapore

[∥]College of Chemistry and Chemical Engineering, Hunan University, Changsha, 410082, People's Republic of China

Supporting Information

ABSTRACT: Organic radicals display unique physical structures and could become next generation functional materials. However, design and synthesis of stable neutral radicals with a significant polyradical character has been an enormous challenge for chemists. In this work, we synthesized a series of stable 3,6-linked, kinetically blocked fluorenyl radical oligomers up to hexamer (**FR-n**, n = 1−6). Their ground-state geometric and electronic structures were systematically studied by various experimental methods including X-ray crystallographic analysis, variable temperature nuclear magnetic resonance, electron spin resonance, and superconducting quantum interference device measurements, supported by density functional theory and *ab initio* calculations. Moderate antiferromagnetic coupling between the fluorenyl radicals was observed, and moderate to large diradical and polyradical characters were calculated from dimer onward. Furthermore, their photophysical properties were estimated by steady-state, transient absorption, and two-photon absorption measurements, and their electrochemical properties were investigated by cyclic voltammetry/differential pulse voltammetry and spectro-electrochemical measurements. A clear chain length dependence of their optical, electrochemical, and magnetic properties was found for the oligomers with an odd or even number of spin centers, respectively.

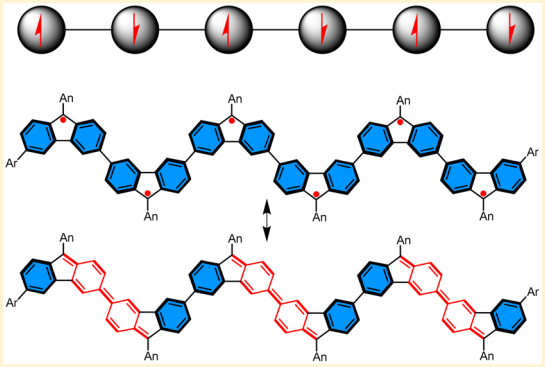

INTRODUCTION

π-Conjugated polycyclic hydrocarbons with an open-shell singlet ground state have recently attracted immense attention due to their unique optical, electronic, and magnetic properties and potential applications in organic electronics, nonlinear optics, spintronics, and energy storage devices.[1] So far, various persistent carbon-centered monoradicals such as polychlorotriphenylmethyls,[2] cyclopentadienyls,[3] and phenalenyls[4] have been designed and synthesized. Connection of two carbon radical centers via a π-conjugated spacer in an antiferromagnetic (AFM) coupling mode could lead to a diradical-like structure in the singlet ground state, which is called an open-shell singlet diradicaloid.[1f,5] Theoretically, a diradical character index (y_0) can be used to account for the bond order of the two frontier π-electrons based on the occupation number of the lowest unoccupied natural orbital (LUNO).[6] Nakano et al. have nicely correlated the diradical character to the excitation energies, nonlinear optical properties, and singlet fission phenomenon in the open-shell singlet diradicaloid systems,[5] which were also validated by recent experimental studies on relatively stable diradicaloids such as bisphenalenyls,[7] quinoidal oligothiophenes and thienacenes,[8] zethrenes,[9] indenofluorenes,[10] anthenes,[11] and extended *para*-quinodimethanes.[12] However, so far there have been very few reports on the stable open-shell polyradicaloids with a low-spin ground state and a significant polyradical character.[13] Organic carbon-centered radicals with a polyradical character, that is, in which multiple π-electrons are not tightly paired into the bonding molecular orbitals, are supposed to be extremely reactive, which makes it more challenging for chemists to design, synthesize, isolate, and characterize stable polyradicaloids. In addition, too strong or too weak AFM coupling between the spins would result in a too small or too large polyradical character, respectively,[13b,c] and thus, a moderate spin−spin coupling is more desirable for optimal physical properties.

Among various carbon-centered monoradicals, cyclopentadienyl radicals as one of the most stable π-conjugated hydrocarbon radicals have been extensively studied and some of them have been isolated in crystalline form.[3] The stability of

Received: August 4, 2016
Published: September 9, 2016

DOI: 10.1021/jacs.6b08138
J. Am. Chem. Soc. 2016, 138, 13048−13058

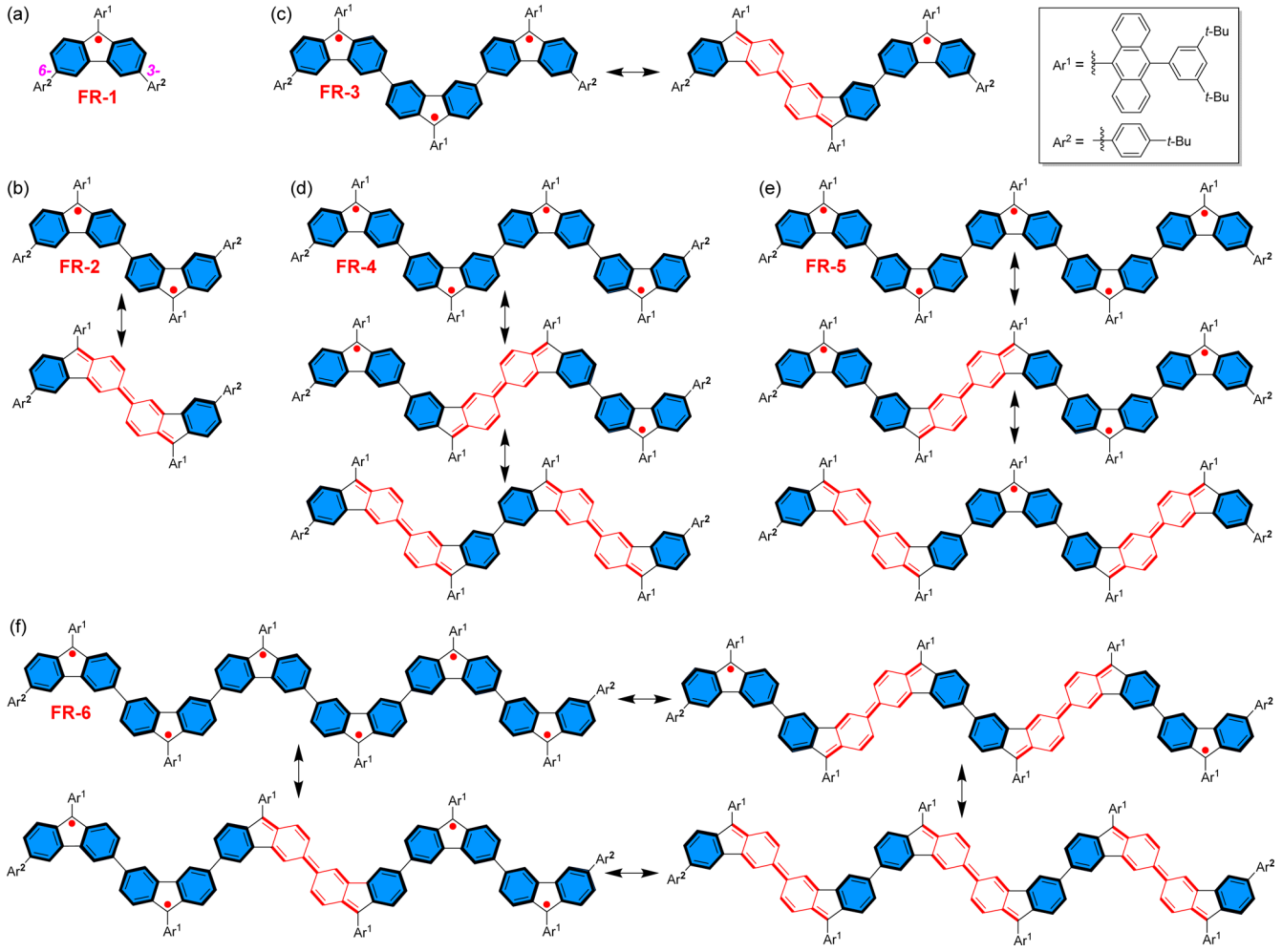

Figure 1. Chemical structures and representative canonical forms of the 3,6-linked fluorenyl radical oligomers.

the cyclopentadienyl radical center can be effectively improved by kinetic blocking and spin delocalization. As a dibenzocyclopentadienyl derivative, the fluorenyl radical is easy to chemically access and has sufficient stability if the 9-position is appropriately substituted. Our group first demonstrated that a 9-anthryl group can effectively stabilize fluorenyl monoradical, and the obtained monoradical and diradicals can be even purified by normal silica gel column chromatography.[14] Kubo's group also reported a series of π-extended fluorenyl monoradicals substituted by 9-anthryl groups, which are stable too.[15] In this context, a series of 3,6-linked fluorenyl radical oligomers **FR-n** (n = 1−6) in which the 9-positions of all fluorenyl radicals are kinetically blocked by 3,5-di-*tert*-butylphenyl substituted 9-anthryl groups are designed and synthesized as potential stable polyradicaloids (Figure 1). The 3,6-linkage allows an efficient AFM coupling between the fluorenyl radicals; that is, a closed-shell quinoidal form can be drawn for the two neighboring fluorenyl radicals (see representative canonical forms in Figure 1; only *trans* forms are drawn). We demonstrated that the recovery of Clar's aromatic sextet rings (the hexagons shaded in blue color in Figure 1) in the diradical canonical form can serve as a major driving force to form diradical, and the more sextets gained, the larger the diradical character.[9c] Taking the dimer **FR-2** as an example, two aromatic sextet rings can be gained from the closed-shell form to the diradical form, and thus, moderate diradical character can be expected for this molecule. Similar analyses can be applied to the higher order oligomers, and there is sufficient driving force (two sextets) from the diradical to tetraradical (in **FR-4**/**FR-5**) and even to hexaradical form (in **FR-6**). Therefore, this series of fluorenyl radical oligomers is expected to be stable and show significant diradical and polyradical character. In this Article, we will report comprehensive studies on their synthesis, ground-state geometric and electronic structures, and chain-length-dependent optical, electrochemical, and magnetic properties by various experimental techniques as well as theoretical methods.

RESULTS AND DISCUSSION

Synthesis. The synthetic approach to six oligoradicals (**FR-n**, n = 1−6) is depicted in Scheme 1. The synthesis of the key building block **4** starts from 9-(3,5-di-*tert*-butylphenyl)-anthracene (**1**)[14] which can be easily converted into 9-bromo-10-(3,5-di-*tert*-butylphenyl)anthracene (**2**) by bromination with NBS in 89% yield. Compound **2** was treated with 0.98 equiv of *n*-BuLi followed by reaction with 3,6-dibromo-9*H*-fluoren-9-one to give the alcohol compound **3** in 81% yield. The alcohol group was then protected by methyl with iodomethane to provide the key building block **4** in 95% yield. Then, the Suzuki coupling reaction between **4** and 0.9 equiv of 4-*tert*-butylphenylboronic acid afforded the monosubstituted compound **5** (in 54% yield) and the disubstituted

DOI: 10.1021/jacs.6b08138
J. Am. Chem. Soc. 2016, 138, 13048−13058

Scheme 1. Synthetic Route for FR-n (n = 1−6)[a]

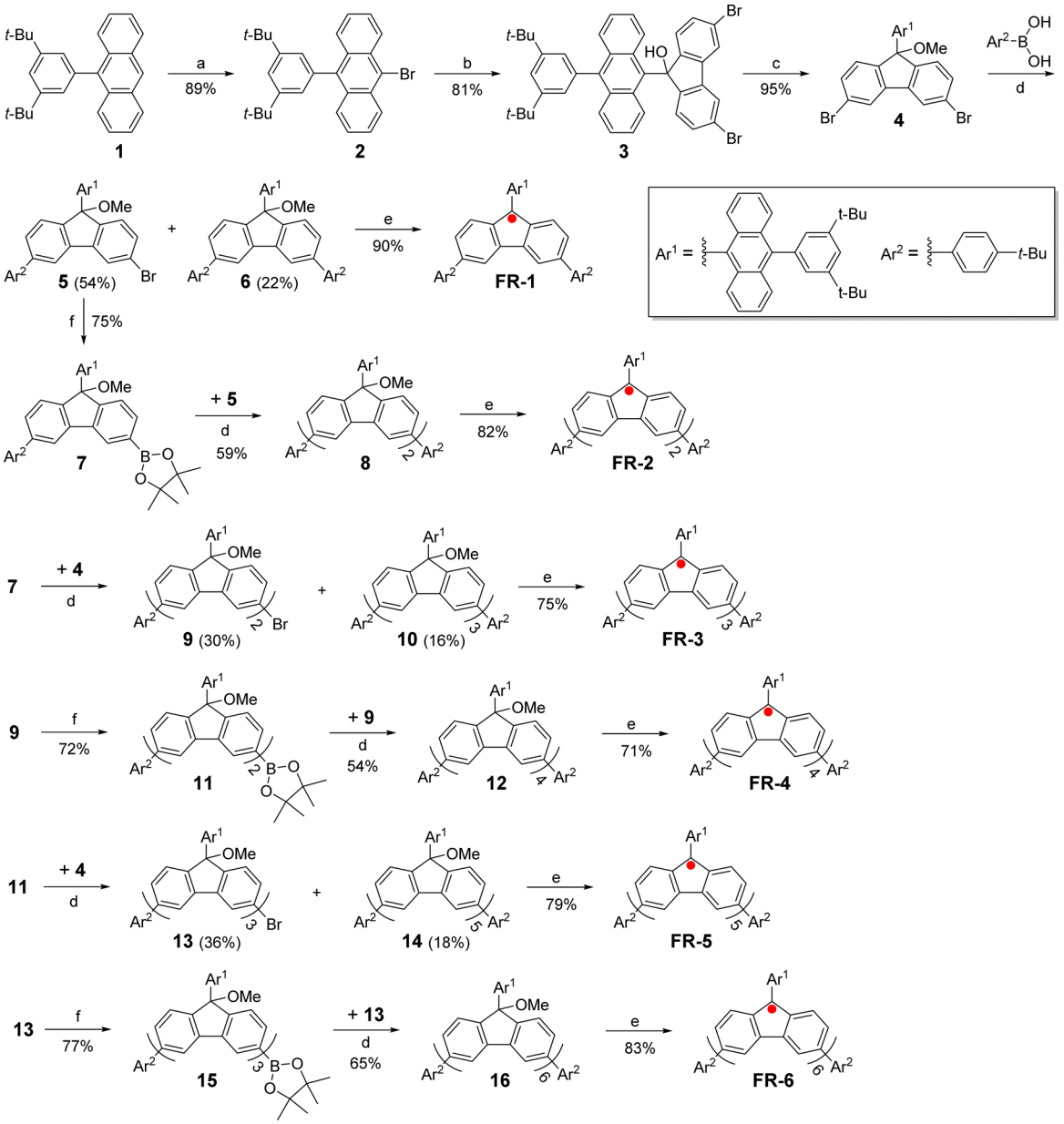

[a]*Reagents and conditions*: (a) NBS, $FeCl_3$ (cat.), $CHCl_3$; (b) (i) *n*-BuLi, THF; (ii) 3,6-dibromofluorenone; (iii) H_2O; (c) NaH, THF, then MeI; (d) $Pd(PPh_3)_4$, K_2CO_3, THF/H_2O, reflux; (e) $SnCl_2$, CH_2Cl_2; (f) $B_2(Pin)_2$, $Pd(dppf)Cl_2CH_2Cl_2$, KOAc, dioxane.

compound **6** (in 22% yield). The monobromo compound **5** was converted into the corresponding boronic ester **7** in 75% yield via palladium catalyzed Miyaura borylation. The Suzuki coupling reaction between **5** and **7** gave the fluorenyl dimer precursor **8** in 59% yield. Following a similar strategy, the monoboronic esters **11** and **13** were prepared, which were used for the synthesis of fluorenyl tetramer and hexamer precursors **12** and **16**, respectively. The trimer and pentamer precursors (**10** and **14**) were isolated during the Suzuki coupling reaction between the monoboronic esters (**7** and **11**) with 1 equiv of **5**. In the last step, the obtained precursors (**6**, **8**, **10**, **12**, **14**, and **16**) were converted into the corresponding radicals **FR-1**, **FR-2**, **FR-3**, **FR-4**, **FR-5**, and **FR-6** by reduction reaction with $SnCl_2$ in dichloromethane (DCM) in nearly quantitative yield (monitored by thin layer chromatography and MALDI-TOF mass spectrometry).[16] Importantly, all of these fluorenyl radical oligomers are stable compounds and can be easily purified by routine silica gel column chromatography, thus facilitating standard structural and physical characterizations. Their MALDI-TOF mass spectra and high-resolution mass spectra (HRMS) were found to be consistent with the target structures (see the Supporting Information). Variable temperature (VT) ^{1}H NMR spectra also supported their structures (*vide infra* and more in the Supporting Information). In addition, the structures of radicals **FR-1** and **FR-2** were further confirmed by X-ray crystallographic analysis (*vide infra*). All of the intermediates were well characterized by ^{1}H and ^{13}C NMR and HRMS, and were found to be consistent with the proposed structures (see the Supporting Information).

X-ray Crystallographic Analysis. Single crystals for **FR-1** and **FR-2** suitable for X-ray crystallographic analysis were grown by slow diffusion of acetonitrile into the toluene

DOI: 10.1021/jacs.6b08138
J. Am. Chem. Soc. 2016, 138, 13048−13058

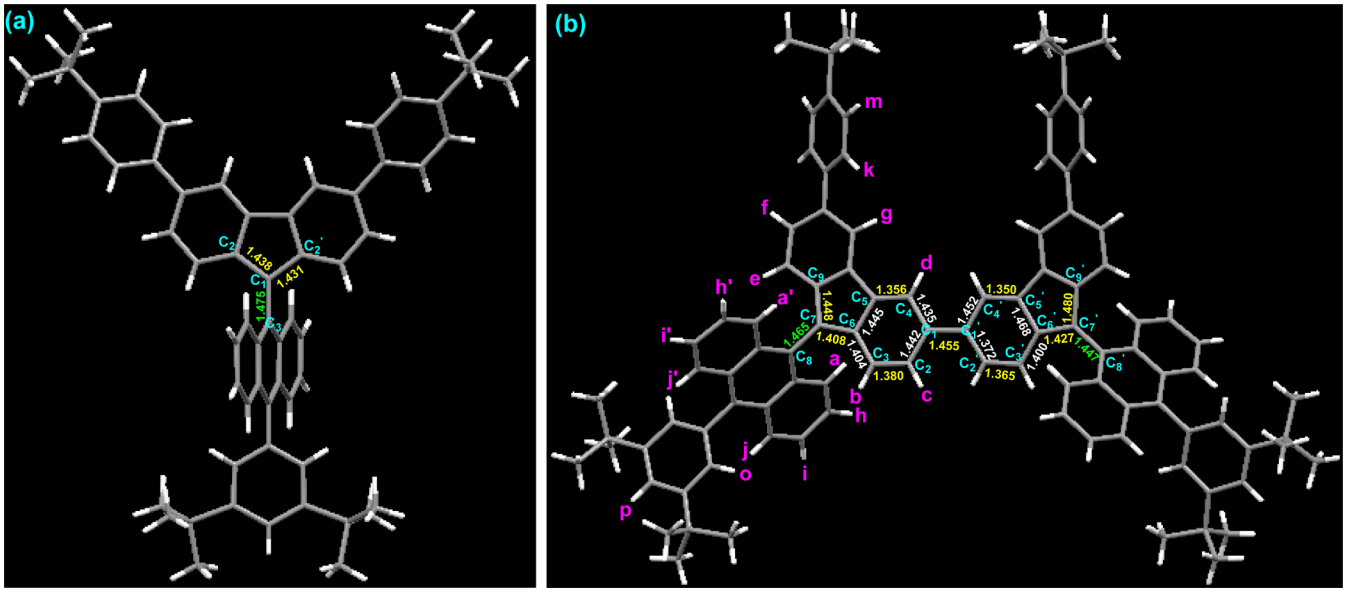

Figure 2. X-ray crystallographic structures of **FR-1** and **FR-2** and selected bond lengths (in Å).

solutions under natural ambient conditions, and their structures are shown in Figure 2.[17] The dihedral angle between the fluorenyl and anthryl moieties in **FR-1** is 80° (mean value), and the almost orthogonal conformation indicates that the 9-anthryl group can be used as a kinetic stabilization group for fluorenyl radicals, and, at the same time, can improve the solubility. However, the dihedral angle between the fluorenyl and anthryl moieties in the crystal **FR-2** is much smaller (59°), presumably due to the contribution of a quinoidal structure in the **FR-2** diradicaloid (Figure 1b). Theoretically, both *cis* and *trans* configurations could exist for **FR-2**, but only *cis* isomer was crystallized. Due to the crystalline packing effects, the bond lengths of the symmetric units are slightly different in both cases. Bond length analysis reveals that the lengths of the C_1-C_2 bond (1.438 Å) and the C_1-C_2' bond (1.431 Å) of the fluorenyl in the crystal **FR-1** are almost the same and have a typical $C(sp^2)-C(sp^2)$ single bond character, but these two bonds of the same position in the crystal of **FR-2** show quite different bond lengths; that is, the length of the C_7-C_9 bond (1.448 Å) is significantly longer than that of the C_6-C_7 bond (1.408 Å), and the length of the $C_7'-C_9'$ bond (1.480 Å) is also significantly longer than that of the $C_6'-C_7'$ bond (1.427 Å). In addition, significant bond length alternation was observed for the two central benzenoid rings, and all of these indicate an AFM bonding between the two spin centers. On the other hand, the length of the C_1-C_1' bond linked to two fluorenyl groups is 1.455 Å, which is much longer than that of the typical olefins (1.33–1.34 Å), implying that there are moderate contributions of both the diradical form and quinoidal form to the ground-state electronic structure, which is in accordance with its moderate diradical character (*vide infra*).

Theoretical Calculations. To further understand the ground-state geometric and electronic structures of these fluorenyl oligomers, density functional theory (DFT) calculations at the UCAM-B3LYP/6-31G (d,p)[18] level were first carried out. To reduce the computational cost, all the *tert*-butyl groups were replaced with hydrogen atoms. Due to the contribution of the quinoidal structures in the **FR-n** (n = 2–6), there could be various *cis*/*trans* isomers for these oligomers. Our calculations show that the *cis* and *trans* isomers have nearly identical energy in **FR-2**. However, the all-*cis* and the *cis*–*trans* isomers have a slightly higher energy (2.5 and 1.6 kcal/mol, respectively) than the all-*trans* isomer in **FR-3** (Figure S1 in the Supporting Information). In cases of the higher order oligomers **FR-4** to **FR-6**, only the all-*trans* isomers were calculated. Our DFT results reveal that the oligomers with an even number of fluorenyl units (**FR-2**, **FR-4**, and **FR-6**) have an open-shell singlet ground state, whereas the oligomers with an odd number of fluorenyl units (**FR-1**, **FR-3**, and **FR-5**) have a doublet ground state. Spin-density maps of these radical oligomers in the ground state show that the fluorenyl radicals nicely interact with each other and the spins are delocalized along the whole π-conjugated frameworks (Figure 3). The diradical character index y_0, tetraradical character index y_1, and hexaradical character index y_2 of **FR-n** (n = 2–6) were calculated on the basis of the occupation number of the LUNO, LUNO+1, and LUNO+2, respectively, according to Yamaguchi's scheme (Table S1 in the Supporting Information).[19] All of the oligoradicals, except monoradical **FR-1**, show moderate to large diradical character values ($y_0 > 0.5$). It is noteworthy that a moderate tetraradical character y_1 for the higher oligoradicals **FR-4** (y_1 = 0.45), **FR5** (y_1 = 0.43), and **FR-6** (y_1 = 0.56) was also calculated. Furthermore, the radical **FR-6** displays a moderate hexaradical character value (y_2 = 0.41). Therefore, it is demonstrated that the higher oligomers have moderate polyradical characters due to the moderate AFM coupling between the fluorenyl radicals.

To better address the polyradical characters and excitation energies of these oligomers, the analysis of the natural orbital occupations was carried out using the restricted active space spin flip method (RAS-SF/6-31G*), which can properly deal with the strongly correlated electrons.[20,9e,13c] The radical characters in the ground state were estimated by the number of unpaired electrons (N_U).[21] Since the calculated occupation numbers of HONO–i and LUNO+i (i = 0–2) also meet the basis of Yamaguchi's scheme: $n_{HONO-i} + n_{LUNO+i} = 2$ (Figure 4 and Figure S2 in the Supporting Information), the multiple radical characters (y_i, i = 0–2) were also calculated by using Yamaguchi's scheme for comparison (Table 1).

DOI: 10.1021/jacs.6b08138
J. Am. Chem. Soc. 2016, 138, 13048–13058

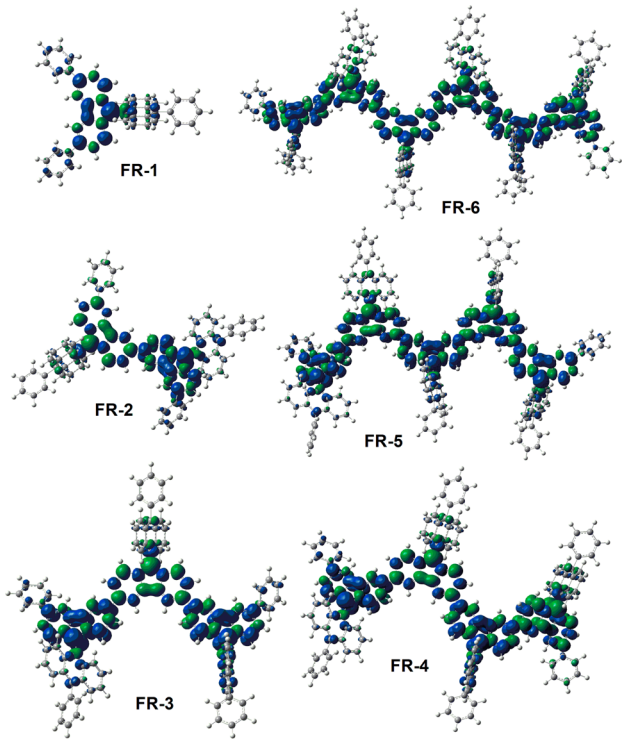

Figure 3. Calculated (UCAM-B3LYP) spin density distributions of the open-shell singlet (**FR-2**, **FR-4**, **FR-6**) or doublet (**FR-1**, **FR-3**, **FR-5**) in all-*trans* forms. Blue and green surfaces represent α and β spin density distributions with 0.004 au isosurfaces, respectively.

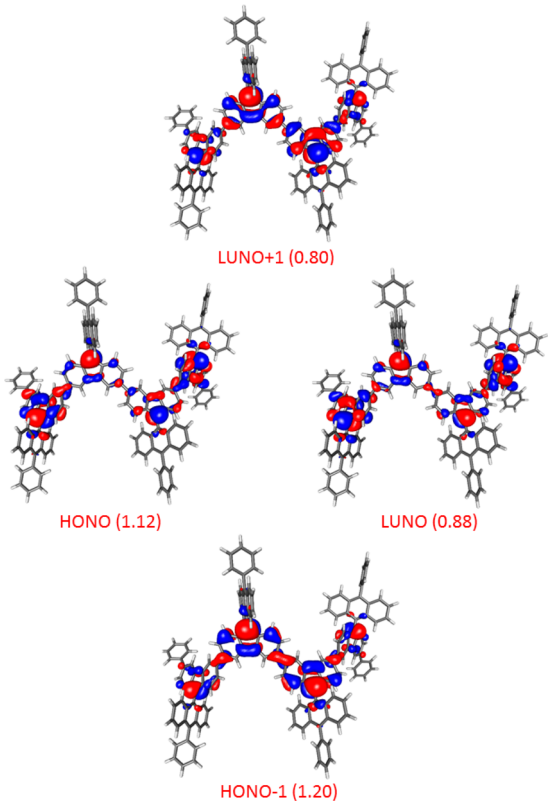

Figure 4. Calculated (RAS-SF) natural orbitals and occupation numbers of **FR-4** (in all-*trans* form) in the singlet ground state.

Table 1. Calculated (RAS-SF/6-31G*) Unpaired Electron Numbers (N_U) and Radical Characters (y_i, i = 0-2) of FR-n (n = 2−6)

molecule	N_U	y_0	y_1	y_2
FR-2	1.65	0.66	0	0
FR-4	3.32	0.75	0.59	0
FR-6	5.05	0.80	0.68	0.59
FR-3	1.95	0.18	0	0
FR-5	3.23	0.28	0.24	0

The NO diagrams and occupancy numbers of **FR-n** (n = 2−6) are shown in Figure 4 and Figure S2 in the Supporting Information. Taking **FR-4** as an example, the unpaired electron density is mainly localized at the four fluorenyl units, indicating its large radical character. Significant occupancy numbers were calculated for the LUNO and LUNO+1, and accordingly, a large N_U value of 3.32 was obtained. Similar results were found for all other oligomers. It was found that the radical character N_U increases in the two series of oligomers as the chain length increases, i.e., series A with an even number (**FR-2**, **FR-4**, and **FR-6**) and series B with an odd number (**FR-3** and **FR-5**) of fluorenyl units, respectively (Table 1). Yamaguchi's polyradical characters (y_i, i = 0−2) calculated by this method show a similar trend (Table 1) and are in agreement with the UCAM-B3LYP calculations (Table S1 in the Supporting Information). Again, **FR-4** and **FR-5** show moderate tetraradical character and **FR-6** even exhibits moderate hexaradical character.

The excitation energies from the low-spin (LS) ground state to the high-spin (HS) excited state were also calculated (Figure 5 and Table S2 in the Supporting Information). In accordance

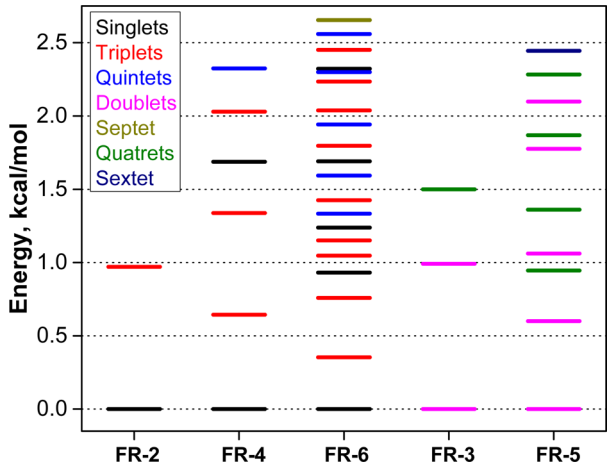

Figure 5. Calculated (RAS-SF) excitation energies from the LS ground state and the HS excited states of **FR-n** (n = 2−6).

with their large radical characters, the calculated vertical energy gaps from the ground state to the lowest excited state are substantially small in these oligomers (<1 kcal/mol), and they also drop with extension of molecular size in both series A and series B. The excitation energies to higher excited states are also not so large, indicating that the molecules could be thermally promoted to even higher spin states.

Magnetic Properties. The ground-state electronic structures of these oligoradicals were further investigated by magnetic measurements such as VT NMR, electron spin resonance (ESR), and superconducting quantum interference device (SQUID) measurements. Monoradical **FR-1** did not

DOI: 10.1021/jacs.6b08138
J. Am. Chem. Soc. 2016, 138, 13048−13058

show any NMR signals for the fluorenyl core at room temperature and even after cooling to 183 K due to its paramagnetic character. The diradicaloid **FR-2** showed broad and weak ^{1}H NMR signals for the fluorenyl core (e.g., protons b, c, and e) at room temperature, while the peaks began to emerge and sharpen upon cooling (Figure 6). At 213 K, sharp

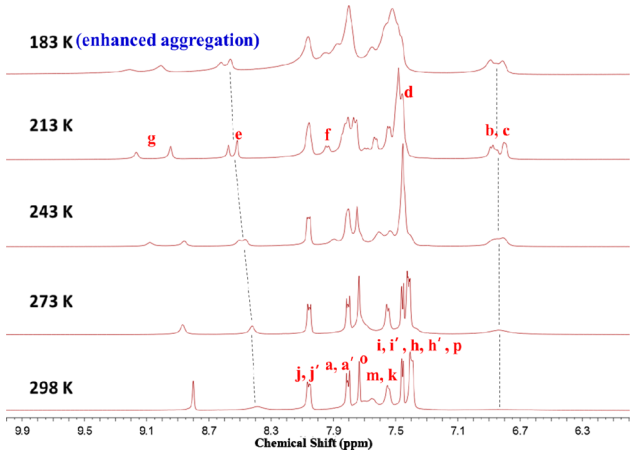

Figure 6. Variable-temperature ^{1}H NMR spectra of **FR-2** in THF-d_8 in the aromatic region and assignment of aromatic protons. The resonance assignment referred to the structure shown in Figure 2.

peaks appeared from the fluorenyl backbone that can be reasonably assigned to the proposed structure. This phenomenon is commonly observed in most previously reported open-shell singlet diradicaloids[9] due to the existence of a significant amount of thermally excited triplet biradical species, which is a little higher in energy than the singlet diradical. Further decrease of temperature to 183 K led to signal broadening due to enhanced aggregation at lower temperature. Similar NMR broadening at room temperature and sharpening as temperature decreases were observed for the higher oligoradicals (Figures S3–S6 in the Supporting Information), but the broadening became more serious for **FR-3** and **FR-5** (due to the odd number of spins) and for **FR-4** and **FR-6** (due to the polyradical character). ESR measurements of all oligoradicals in toluene displayed strong signals at room temperature even at low temperature (−90 °C in toluene) with g_e = 2.0026 (Figure S7 in the Supporting Information), and the signal intensity gradually decreases as the temperature decreases, indicating that they all have a low-spin (singlet or doublet) ground state. The spin concentration of **FR-n** (n = 2–6) was estimated to be 0.07, 0.83, 0.17, 0.56, and 0.42, respectively, by using the monoradical **FR-1** as a standard. It is found that the oligomers with an odd number of fluorenyl units show a larger spin concentration than those with an even number of fluorenyl units. From **FR-2** to **FR-4** and to **FR-6**, the spin contraction increases as a consequence of the increased diradical and polyradical characters. From **FR-1** to **FR-3** and to **FR-5**, however, the spin concentration decreases presumably due to certain intermolecular or intramolecular spin–spin association in solution.

SQUID measurements were performed with the powder samples of **FR-n** (n = 1–6) at 2–380 K (Figure 7), and estimated excitation energies from the LS ground state to the first HS excited state are collected in Table 2. For the monomer **FR-1**, the product of the molar magnetic susceptibility (χ_M) by the temperature (T, in K) gave a value of 0.36 emu·K·mol^{-1} from 25 to 400 K, which is close to the theoretical spin only value (0.375 emu·K·mol^{-1}) for an S = 1/2 system. The product χ_M·T drops at temperatures below 25 K as a result of weak intermolecular AFM coupling. For the dimer **FR-2**, the χ_M·T increases after 150 K and fitting of the data using the Bleaney–Bowers equation[22a] based on a singlet–triplet model gave a singlet–triplet energy gap (ΔE_{S-T}) of −3.52 kcal/mol with a singlet ground state. A similar trend was observed for the tetramer **FR-4** and hexamer **FR-6**, and both have a singlet

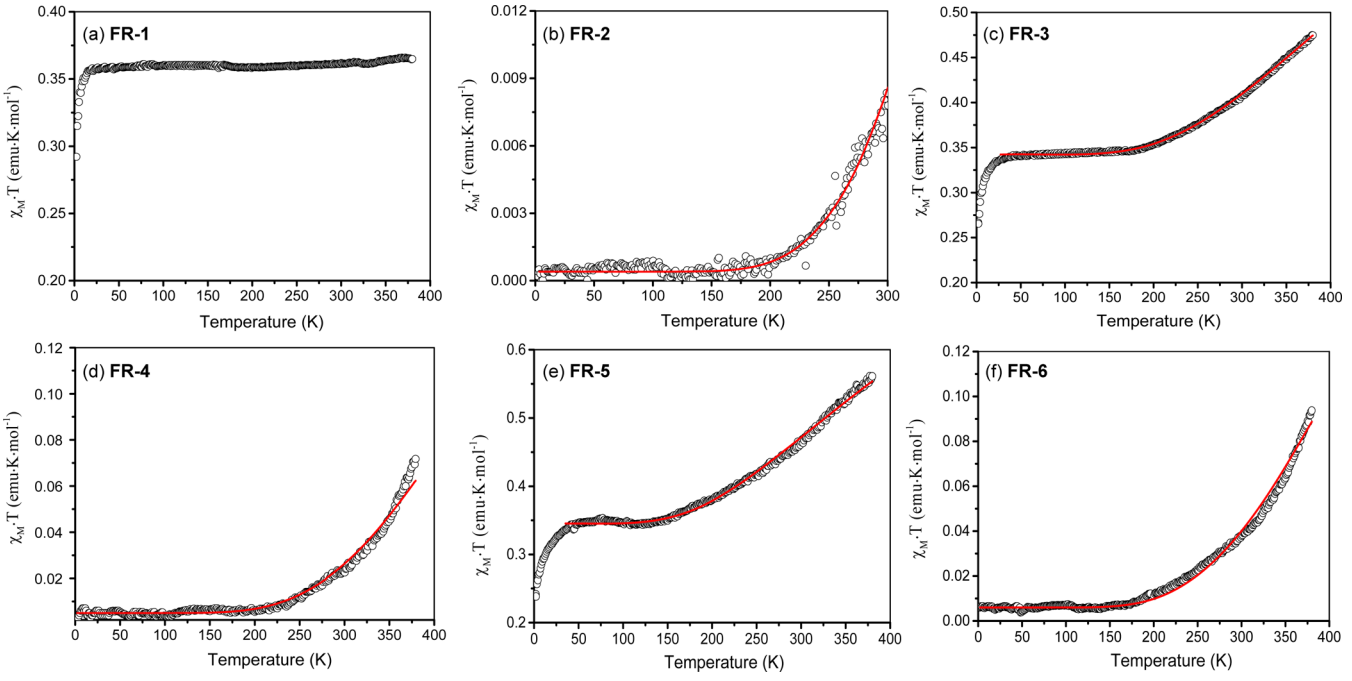

Figure 7. $\chi_M T$–T curves in the SQUID measurements for the solids of **FR-n** (n = 1–6). The solid lines are the fitting curves according to the Bleaney–Bowers equation for **FR-2**/**FR-4**/**FR-6** and the trimer model for **FR-3**/**FR-5**; the g-factor was taken to be 2.00.

DOI: 10.1021/jacs.6b08138
J. Am. Chem. Soc. 2016, 138, 13048–13058

Table 2. Photophysical, Electrochemical, and Magnetic Properties of FR-n (n = 1−6)[a]

molecule	λ_{abs} (nm)	ε_{max} (M^{-1} cm^{-1})	τ (ps)	$\sigma^{(2)}{}_{max}$ (GM)	$E_{1/2}{}^{ox}$ (V)	$E_{1/2}{}^{red}$ (V)	E_{HOMO} (eV)	E_{LUMO} (eV)	$E_g{}^{EC}$ (eV)	$E_g{}^{opt}$ (eV)	ΔE_{LS-HS} (kcal/mol)
FR-1	394	1.63×10^4	0.30	300	0.12	−1.10	−4.85	−3.75	1.10	1.27	
	544	0.43×10^4									
	587	0.34×10^4									
	768	0.08×10^4									
FR-2	394	1.72×10^4	1.30	600	0.17	−1.13	−4.90	−3.73	1.17	1.33	−3.52
	597	1.24×10^4			0.31	−1.32					
	745	1.91×10^4									
FR-3	396	3.24×10^4	1.00	1100	0.05	−1.01	−4.77	−3.87	0.90	1.24	−2.19
	599	1.83×10^4			0.32	−1.20					
	755	2.08×10^4			0.46	−1.44					
	955	1.13×10^4									
FR-4	394	2.74×10^4	0.50	1500	0.13	−1.09	−4.83	−3.82	1.01	1.26	−2.94
	594	1.92×10^4			0.45	−1.30					
	735	2.21×10^4				−1.49					
FR-5	395	3.56×10^4	0.45	1800	0.00	−1.01	−4.65	−3.88	0.77	1.21	−1.76
	600	2.23×10^4			0.16	−1.10					
	755	2.43×10^4			0.30	−1.24					
	968	1.42×10^4			0.47	−1.40					
						−1.55					
FR-6	395	3.56×10^4	0.40	1800	0.02	−1.07	−4.74	−3.82	0.92	1.23	−2.65
	598	2.43×10^4			0.15	−1.18					
	739	2.64×10^4			0.26	−1.30					
					0.38	−1.46					
					0.47	−1.55					

[a] λ_{abs}: absorption maximum measured in toluene. ε_{max}: molar extinction coefficient at the absorption maximum. τ is the singlet excited state lifetime obtained from TA. $E_{1/2}{}^{ox}$ and $E_{1/2}{}^{red}$ are half-wave potentials of the oxidative and reductive waves, respectively, with potentials vs Fc/Fc^+ couple. HOMO and LUMO energy levels were calculated according to the equations $E_{HOMO} = -(4.8 + E_{ox}{}^{onset})$ and $E_{LUMO} = -(4.8 + E_{red}{}^{onset})$, where $E_{ox}{}^{onset}$ and $E_{red}{}^{onset}$ are the onset potentials of the first oxidative and reductive redox wave, respectively. $E_g{}^{EC}$: electrochemical energy gap derived from $E_{LUMO}-E_{HOMO}$. $E_g{}^{opt}$: optical energy gap derived from lowest energy absorption onset in the absorption spectra. ΔE_{LS-HS}: the energy difference between the LS ground state and the first HS excited state estimated from SQUID measurements. $\sigma^{(2)}{}_{max}$ is the maximum TPA cross section at a wavelength of 1500 nm.

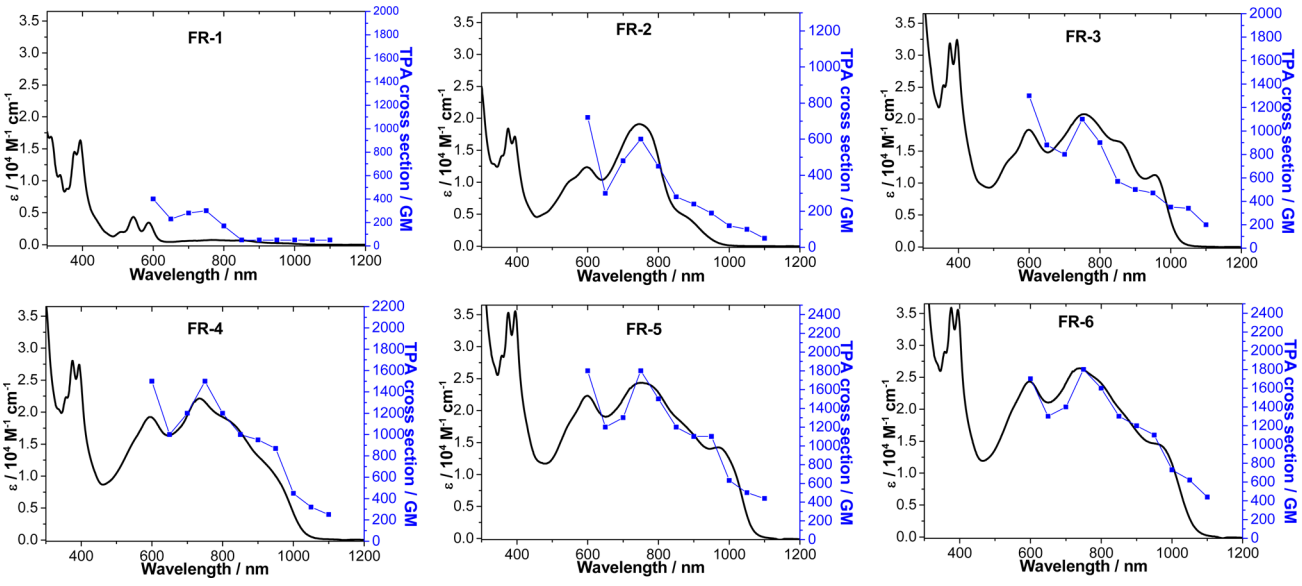

Figure 8. One-photon and two-photon absorption spectra of **FR-n** (n = 1−6). The spectra were recorded in toluene. TPA spectra are plotted at λ_{ex}/2.

ground state, with an estimated ΔE_{S-T} value of −2.94 and −2.65 kcal/mol, respectively. For the trimer **FR-3** and pentamer **FR-5**, due to the existence of an odd number of spins, a constant $\chi_M \cdot T$ value of around 0.35 emu·K·mol^{-1} was observed between 25 and 125 K, followed by a $\chi_M \cdot T$ increase with increase of temperature due to the thermal population from the doublet ground state to the quartet excited state. The energy gaps were estimated as −2.91 and −1.76 kcal/mol, respectively, by fitting the data with the linear trimer model.[22b] Similar to the monomer, weak intermolecular AFM coupling

DOI: 10.1021/jacs.6b08138
J. Am. Chem. Soc. 2016, 138, 13048−13058

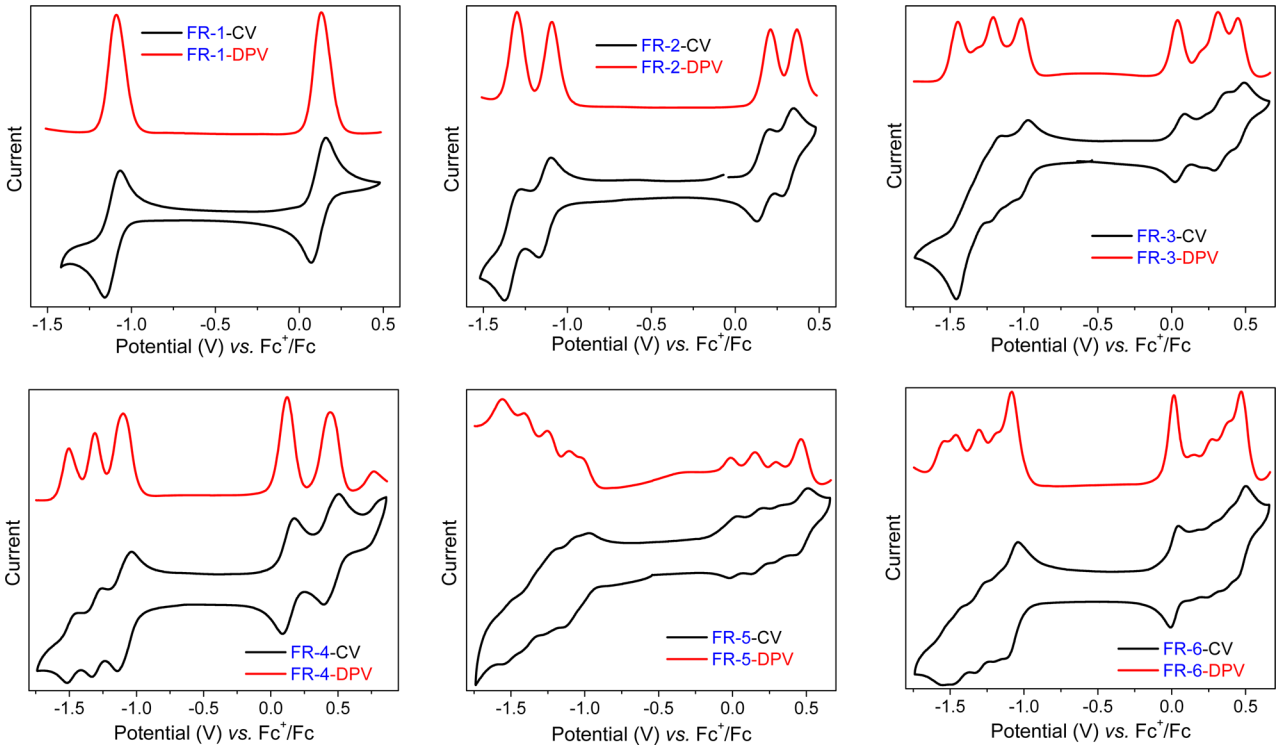

Figure 9. Cyclic voltammograms (black curves) and differential pulse voltammograms (red curves) of **FR-n** (n = 1−6) in DCM solutions.

was observed below 25 K. Therefore, for the oligomers with either an even or odd number of fluorenyl units, the measured energy gaps from the LS ground state to the HS excited state decrease with the increase of molecular length, in consistency with their calculated radical characters and vertical energy gaps.

Optical Properties. The UV−vis−NIR spectra of this series of fluorenyl-based oligoradicals were measured in toluene (Figure 8 and Figure S8 in the Supporting Information) at a concentration of ca. 1×10^{-5} M, which exhibit different one-photon absorption (OPA) spectral features as the number of spin centers increases, and the corresponding photophysical data are listed in Table 2. The **FR-1** displayed an intense absorption band with vibronic splitting in the region of 300−400 nm, which is characteristic of that of anthracene.[23] A long weak absorption tail into the near-infrared (NIR) region was observed due to the existence of one unpaired electron and is similar to our previously reported fluorenyl monoradical analogue.[14] In contrast, the absorption spectrum of **FR-2** showed a relatively intense band in the NIR region with λ_{max} = 720 nm along with a shoulder at 850 nm extending up to 1000 nm, which is quite different from that of monoradical **FR-1**, indicating that there is significant AFM coupling interaction between the two radicals. The **FR-3** also displayed a relatively intense band in the NIR region as observed in **FR-2**. It is worth noting that **FR-3** exhibited a broader spectral response extending up to 1050 nm with a bathochromic shift of 50 nm compared to that of **FR-2**, further indicating that there are also significant spin coupling interactions between the three radicals. This optical feature was entirely observed in further higher oligomers **FR-4**, **FR-5**, and **FR-6**. Generally, the absorption spectra and extinction coefficients of the radicals are continuously red-shifted and increased, respectively, as the number of radicals increases, all indicating multiple AFM spin interactions in the ground state. The optical energy gaps (E_g^{opt}) of **FR-n** (n = 1−6) were roughly estimated to be 1.27, 1.33, 1.24, 1.26, 1.21, and 1.23 eV, respectively, from the lowest energy absorption onset. Therefore, the optical energy gap decreases with the extension of chain length in each individual series containing an even number (**FR-2**, **FR-4**, and **FR-6**) or an odd number (**FR-1**, **FR-3**, and **FR-5**) of fluorenyl units. A more accurate chain length dependence will be discussed on the basis of electrochemical energy gaps.

As it is known that an open-shell radical character can enhance the two-photon absorption (TPA) cross section,[24] TPA measurements were conducted for oligoradicals **FR-n** (n = 1−6) by using the open aperture Z-scan method in the wavelength range from 1200 to 2200 nm where one-photon absorption contribution is negligible (Figure 8, Table 2, and Figure S9 in the Supporting Information). The monoradical **FR-1** displayed significant TPA response in the region 1200−1600 nm with a maximum TPA cross section value ($\sigma^{(2)}_{max}$) of 300 GM at 1500 nm. The higher order oligoradicals **FR-n** (n = 2−6) exhibited a much broader TPA response region extending up to 2200 nm, with $\sigma^{(2)}_{max}$ = 600, 1100, 1500, 1800, and 1800 GM at 1500 nm, respectively. Therefore, $\sigma^{(2)}_{max}$ follows the order **FR-1** < **FR-2** < **FR-3** < **FR-4** < **FR-5** ≈ **FR-6**, and this trend may be correlated to the resonance enhancement of the transitions observed in the OPA spectra and the multiple moderate AFM spin coupling interactions in the higher oligomers. However, the TPA cross section almost reaches saturation at the pentamer.

To investigate the excited-state dynamics of these oligoradicals, the femtosecond transient absorption (TA) measurements were carried out in toluene at room temperature (Figure S10 in the Supporting Information and Table 2). The TA spectra of **FR-1** exhibited ground-state bleaching (GSB) signals around 530−590 nm as well as two relatively higher intensity excited-state absorption (ESA) bands in the 450−530 and 620−750 nm regions (Figure S10 in the Supporting Information). The excited-state lifetime (τ) was determined

DOI: 10.1021/jacs.6b08138
J. Am. Chem. Soc. 2016, 138, 13048−13058

to be 300 fs in the decay profile. This ultrafast excited-state lifetime of **FR-1** is considered to reflect an acceleration of the nonradiative decay rates arising from the smaller energy gap between the lowest excited state and the open-shell ground state. The nonfluorescent property of radical **FR-1** is also well in agreement with its ultrafast excited-state lifetime. The higher oligoradicals **FR-n** (n = 2−6) showed similar TA spectral features with each other. The TA spectra of **FR-n** (n = 2−6) displayed ground-state bleaching (GSB) signals from 530 to 850 nm as well as one relatively weaker intensity ESA band in the region of 450−530 nm, which is distinctly different from **FR-1**. These results are well matched with the steady-state absorptions. Furthermore, ultrafast excited state lifetimes with time constants of 1300, 1000, 500, 450, and 400 fs were observed in the decay profiles of **FR-n** (n = 2−6), respectively. Thus, the excited-state lifetimes decrease as the chain length increases, which might be a consequence of the increased diradical and polyradical characters.

Electrochemical Properties. To investigate the electrochemical properties of these oligomers, cyclic voltammetry and differential pulse voltammetry measurements were carried out in a typical three-electrode electrochemical cell in a solution of tetrabutylammonium hexafluorophosphate (0.1 M) in dry DCM with a scan rate of 50 mV s^{-1} (Figure 9 and Table 2). The monoradical **FR-1** exhibited one reversible oxidation wave at $E_{1/2}^{ox}$ = 0.12 V (vs Fc^+/Fc) and one reversible reduction wave at $E_{1/2}^{red}$ = −1.10 V (vs Fc^+/Fc), which can be correlated to the cation and anion formation. **FR-2** showed two reversible oxidation waves with $E_{1/2}^{ox}$ = 0.17 and 0.31 V and two reversible reduction waves with $E_{1/2}^{red}$ = −1.13 and −1.32 V, indicating that it can be reversibly oxidized to its radical cation and dication, and reduced into radical anion and dianion. Analogously, **FR-3** displayed three reversible oxidation waves with $E_{1/2}^{ox}$ = 0.05, 0.32, and 0.46 V and three quasi-reversible reduction waves with $E_{1/2}^{red}$ = −1.01, −1.20, and −1.44 V, implying that it can be oxidized to its diradical cation, radical dication, and trication, and reduced into diradical anion, radical dianion, and trianion forms. The higher oligoradicals **FR-4**−**FR-6** demonstrated more reductive and oxidative waves due to the diminished Coulomb charge repulsion in the more extended systems. **FR-4** could be reversibly oxidized into diradical dication and tetracation via two-electron transfer at $E_{1/2}^{ox}$ = 0.13 and 0.45 V and reduced into diradical dianion, radical trianion, and tetraanion at $E_{1/2}^{red}$ = −1.09, −1.30, and −1.49 V. For pentamer **FR-5**, four major oxidation processes and five reduction processes were detected, and for hexamer **FR-6**, five major quasi-reversible oxidation processes and five reduction processes were detected.

The HOMO and LUMO energy levels of these oligomers were determined from the onset potentials of the first oxidation and reduction waves, and the electrochemical energy gaps (E_g^{EC} = LUMO−HOMO) thus can be determined accordingly, which are in good accordance with the optical energy gaps (Table 2). It is worth noting that good chain-length dependences of the HOMO/LUMO energy levels and E_g^{EC} were found separately for the oligomers with either an even (series A) or odd number (series B) of fluorenyl units. In each series, with the extension of the chain length, the HOMO energy level increases and the LUMO energy level decreases, leading to a convergence of the E_g^{EC} value. Two linear $E_g^{EC} \sim 1/n$ plots (n is the number of fluorenyl units) were found for these two series (Figure 10), which is similar to many other π-conjugated oligomers.[25] The oligomers with an even and odd number of spins are quite

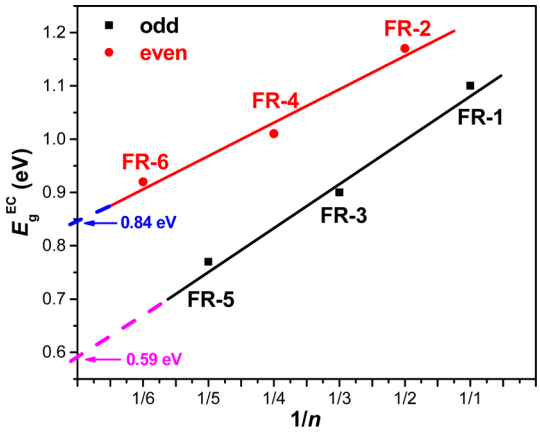

Figure 10. Chain-length (n) dependence of the electrochemical energy gaps (E_g^{EC}) for **FR-n** (n = 1−6). Extrapolation of the linear plot to $n = \infty$ gives the estimated energy gaps for the infinite polymers with odd (black line) or even (red line) spins.

different from each other due to their different electronic structures. Linear extrapolation of the two plots to $n = \infty$ implies that the corresponding infinite polymers with an even and odd number of fluorenyl radicals may have an electrochemical energy gap of 0.84 and 0.59 eV, respectively. This, however, may not be true as, like other conjugated polymers, a saturation of the energy gap could be observed at a certain effective conjugation length.

The multiple-step amphoteric redox behavior of these oligomers allows us to probe their charged states either by electrochemical or chemical oxidation/reduction. Spectroelectrochemical measurements were first conducted in dry DCM solutions, and the absorption spectra of the major oxidized species at different electrode potentials (vs Fc^+/Fc) are shown in Figure 11. **FR-1** can be easily oxidized into a cation, with a broad and intense absorption with λ_{max} at 1075 nm. **FR-2** is oxidized to the radical cation at 0.3 V, with two intense absorption bands in the NIR region (λ_{max} = 1245, 2200 nm), and then further oxidized into dication at 0.8 V (λ_{max} = 1166 nm). **FR-3** can be oxidized into diradical cation at 0.2 V (λ_{max} = 2128 nm), radical dication at 0.4 V (λ_{max} = 1243, 2152 nm), and then trication at 0.9 V (λ_{max} = 1160 nm). In accordance with the CV data, **FR-4** undergoes two-electron oxidation to diradical dication at 0.4 V (λ_{max} = 1110, 1670, 2340 nm) and then two-electron oxidation to the tretracation at 0.9 V (λ_{max} = 1195 nm). **FR-5** can be oxidized to tetraradical cation at 0.3 V (λ_{max} = 1204, 1790 nm) and then multiple electron transfer to the final pentacation at 0.9 V (λ_{max} = 1192 nm). Similarly, **FR-6** is oxidized into pentaradical cation at 0.4 V (λ_{max} = 1030, 1680 nm) and then to hexacation at 1.0 V (λ_{max} = 1195 nm). In general, all of the full oxidized cations show a similar band structure and absorption wavelength, and intermediate radical cations exhibit very long wavelength absorption extending to 3000 nm, indicating their mixed-valence character. It turned out that electrochemical reduction did not have good control on the reduction process; therefore, chemical reduction of these oligomers was conducted in dry DCM and followed by UV−vis−NIR spectroscopic measurements. Using a strong reductant such as KO_2 together with 18-crown-8 gave fully reduced anions, and all of them show a very similar band structure with an absorption maximum at 384 nm, correlated to the absorption of an aromatic fluorenyl anion (Figure S11 in the Supporting Information). The reductions of **FR-n** (n = 2−6) by

DOI: 10.1021/jacs.6b08138
J. Am. Chem. Soc. 2016, 138, 13048−13058

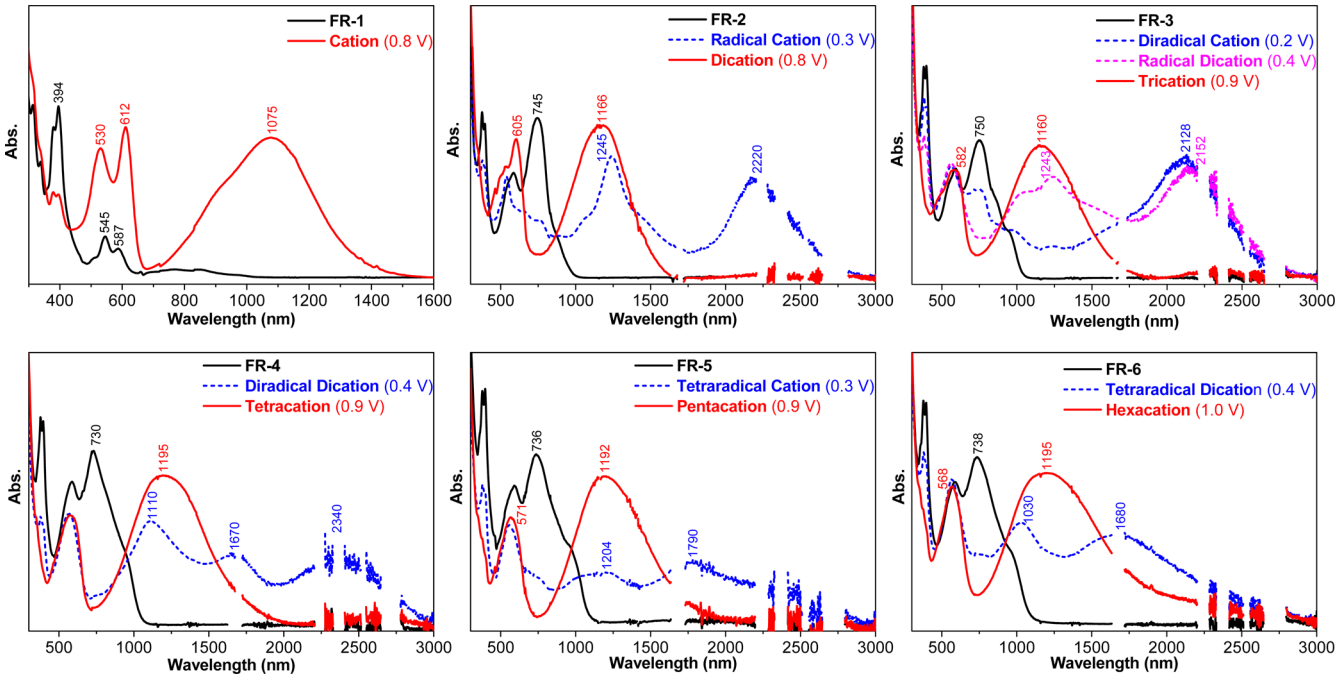

Figure 11. UV−vis−NIR spectra of neutral and oxidized species of **FR-n** (n = 1−6) during the spectro-electrochemical measurements. The applied potential is vs $E(Fc^+/Fc)$.

$CoCp_2$ in DCM stopped at the (multiple)radical monoanions stage, which all show a broad NIR absorption band with λ_{max} = 1947, 1979, 2340, 1866, and 1869 nm, respectively (Figure S12 in the Supporting Information).

CONCLUSIONS

In conclusion, a series of 3,6-linked fluorenyl radical oligomers were synthesized by stepwise reactions. They are exceptionally stable mainly due to kinetic blocking by the bulky anthryl groups. Moderate intramolecular AFM coupling between the radical centers was observed, which leads to moderate polyradical characters, low excitation energies, long wavelength one-photon absorption, large TPA cross sections, and multiple-stage amphoteric redox behavior. Clear chain-length dependence of physical properties can be seen for this unique polyradical-like system. Our research provides a general design strategy for open-shell low-spin systems with polyradical character, which open the opportunities to access stable organic materials with unique optical, electronic, and magnetic properties.

ASSOCIATED CONTENT

Supporting Information

The Supporting Information is available free of charge on the ACS Publications website at DOI: 10.1021/jacs.6b08138.

Synthetic procedures and characterization data of all new compounds, details for all physical characterizations and theoretical calculations, and additional spectroscopic and X-ray crystallographic data (PDF)

Crystallographic information file for **FR-1** (CIF)

Crystallographic information file for **FR-2** (CIF)

AUTHOR INFORMATION

Corresponding Authors

*dongho@yonsei.ac.kr

*chmwuj@nus.edu.sg

Notes

The authors declare no competing financial interest.

ACKNOWLEDGMENTS

J.W. acknowledges financial support from the MOE Tier 3 programme (MOE2014-T3-1-004) and MOE Tier 2 grant (MOE2014-T2-1-080). The work at Yonsei University was supported by the Global Frontier R&D Program on Center for Multiscale Energy System funded by the National Research Foundation under the Ministry of Science, ICT & Future, Korea (NRF-2014M3A6A7060583). Z.Z. acknowledges the financial support from the Startup Fund (531109020043) from Hunan University. We thank Dr Bruno Donnadieu for X-ray crystallographic analysis.

REFERENCES

(1) (a) Sun, Z.; Ye, Q.; Chi, C.; Wu, J. *Chem. Soc. Rev.* **2012**, *41*, 7857. (b) Shimizu, A.; Hirao, Y.; Kubo, T.; Nakano, M.; Botek, E.; Champagne, B. *AIP Conf. Proc.* **2009**, *1504*, 399. (c) Abe, M. *Chem. Rev.* **2013**, *113*, 7011. (d) Sun, Z.; Zeng, Z.; Wu, J. *Acc. Chem. Res.* **2014**, *47*, 2582. (e) Kubo, T. *Chem. Rec.* **2015**, *15*, 218. (f) Zeng, Z.; Shi, X.; Chi, C.; López Navarrete, J. T.; Casado, J.; Wu, J. *Chem. Soc. Rev.* **2015**, *44*, 6578. (g) Kubo, T. *Chem. Lett.* **2015**, *44*, 111.

(2) (a) Ballester, M. *Acc. Chem. Res.* **1985**, *18*, 380. (b) Veciana, J.; Ratera, I. Polychlorotriphenylmethyl radicals: towards multifunctional molecular materials. In *Stable Radicals*; Hicks, R. G., Eds.; John Wiley & Sons, Ltd: Wiltshire, U.K., 2010; Chapter 2, p 33.

(3) (a) Sitzmann, H.; Boese, R. *Angew. Chem., Int. Ed. Engl.* **1991**, *30*, 971. (b) Sitzmann, H.; Bock, H.; Boese, R.; Dezember, T.; Havlas, Z.; Kaim, W.; Moscherosch, M.; Zanathy, L. *J. Am. Chem. Soc.* **1993**, *115*, 12003. (c) Jux, N.; Holczer, K.; Rubin, Y. *Angew. Chem., Int. Ed. Engl.* **1996**, *35*, 1986.

(4) Morita, Y.; Nishida, S. Phenalenyls, cyclopentadienyls, and other carbon-centered radicals. In *Stable Radicals*; Hicks, R. G., Ed.; John Wiley & Sons, Ltd: Wiltshire, U.K., 2010; Chapter 3, p 81.

(5) Nakano, M. *Excitation Energies and Properties of Open-Shell Singlet Molecules*; Springer: New York, 2014.

DOI: 10.1021/jacs.6b08138
J. Am. Chem. Soc. 2016, 138, 13048−13058

(6) (a) Yamaguchi, K.; Fueno, T.; Fukutome, H. *Chem. Phys. Lett.* **1973**, *22*, 461. (b) Yamaguchi, K. In *Self-Consistent Field: Theory and Applications*; Carbo, R., Klobukowski, M., Eds.; Elsevier: Amsterdam, The Netherlands, 1990; p 727.
(7) (a) Ohashi, K.; Kubo, T.; Masui, T.; Yamamoto, K.; Nakasuji, K.; Takui, T.; Kai, Y.; Murata, I. *J. Am. Chem. Soc.* **1998**, *120*, 2018. (b) Kubo, T.; Sakamoto, M.; Akabane, M.; Fujiwara, Y.; Yamamoto, K.; Akita, M.; Inoue, K.; Takui, T.; Nakasuji, K. *Angew. Chem., Int. Ed.* **2004**, *43*, 6474. (c) Kubo, T.; Shimizu, A.; Sakamoto, M.; Uruichi, M.; Yakushi, K.; Nakano, M.; Shiomi, D.; Sato, K.; Takui, T.; Morita, Y.; Nakasuji, K. *Angew. Chem., Int. Ed.* **2005**, *44*, 6564. (d) Shimizu, A.; Uruichi, M.; Yakushi, K.; Matsuzaki, H.; Okamoto, H.; Nakano, M.; Hirao, Y.; Matsumoto, K.; Kurata, H.; Kubo, T. *Angew. Chem., Int. Ed.* **2009**, *48*, 5482. (e) Shimizu, A.; Kubo, T.; Uruichi, M.; Yakushi, K.; Nakano, M.; Shiomi, D.; Sato, K.; Takui, T.; Hirao, Y.; Matsumoto, K.; Kurata, H.; Morita, Y.; Nakasuji, K. *J. Am. Chem. Soc.* **2010**, *132*, 14421. (f) Shimizu, A.; Hirao, Y.; Matsumoto, K.; Kurata, H.; Kubo, T.; Uruichi, M.; Yakushi, K. *Chem. Commun.* **2012**, *48*, 5629.
(8) (a) Takahashi, T.; Matsuoka, K. I.; Takimiya, K.; Otsubo, T.; Aso, Y. *J. Am. Chem. Soc.* **2005**, *127*, 8928. (b) Ponce Ortiz, R.; Casado, J.; Hernandez, V.; López Navarrete, J. T.; Viruela, P. M.; Orti, E.; Takimiya, K.; Otsubo, T. *Angew. Chem., Int. Ed.* **2007**, *46*, 9057. (c) Canesi, E. V.; Fazzi, D.; Colella, L.; Bertarelli, C.; Castiglioni, C. *J. Am. Chem. Soc.* **2012**, *134*, 19070. (d) Rudebusch, G. E.; Fix, A. G.; Henthorn, H. A.; Vonnegut, C. L.; Zakharov, L. N.; Haley, M. M. *Chem. Sci.* **2014**, *5*, 3627. (e) Shi, X.; Burrezo, P. M.; Lee, S.; Zhang, W.; Zheng, B.; Dai, G.; Chang, J.; López Navarrete, J. T.; Huang, K.-W.; Kim, D.; Casado, J.; Chi, C. *Chem. Sci.* **2014**, *5*, 4490. (f) Streifel, B. C.; Zafra, J. L.; Espejo, G. L.; Gómez-García, C. J.; Casado, J.; Tovar, J. D. *Angew. Chem., Int. Ed.* **2015**, *54*, 5888. (g) Shi, X.; Quintero, E.; Lee, S.; Jing, L.; Herng, T. S.; Zheng, B.; Huang, K.-W.; López Navarrete, J. T.; Ding, J.; Kim, D.; Casado, J.; Chi, C. *Chem. Sci.* **2016**, *7*, 3036. (h) Dong, S.; Herng, T. S.; Gopalakrishna, T. Y.; Phan, H.; Lim, Z. L.; Hu, P.; Webster, R. D.; Ding, J.; Chi, C. *Angew. Chem., Int. Ed.* **2016**, *55*, 9316.
(9) (a) Sun, Z.; Huang, K.-W.; Wu, J. *J. Am. Chem. Soc.* **2011**, *133*, 11896. (b) Li, Y.; Heng, K.-W.; Lee, B. S.; Aratani, N.; Zafra, J. L.; Bao, N.; Lee, R.; Sung, Y. M.; Sun, Z.; Huang, K.-W.; Webster, R. D.; López Navarrete, J. T.; Kim, D.; Osuka, A.; Casado, J.; Ding, J.; Wu, J. *J. Am. Chem. Soc.* **2012**, *134*, 14913. (c) Sun, Z.; Lee, S.; Park, K.; Zhu, X.; Zhang, W.; Zheng, B.; Hu, P.; Zeng, Z.; Das, S.; Li, Y.; Chi, C.; Li, R.; Huang, K.; Ding, J.; Kim, D.; Wu, J. *J. Am. Chem. Soc.* **2013**, *135*, 18229. (d) Zeng, W. D.; Sun, Z.; Herng, T. S.; Gonçalves, T. P.; Gopalakrishna, T. Y.; Huang, K.-W.; Ding, J.; Wu, J. *Angew. Chem., Int. Ed.* **2016**, *55*, 8615. (e) Huang, R.; Phan, H.; Herng, T. S.; Hu, P.; Zeng, W.; Dong, S.; Das, S.; Shen, Y.; Ding, J.; Casanova, D.; Wu, J. *J. Am. Chem. Soc.* **2016**, *138*, 10323.
(10) (a) Chase, D. T.; Rose, B. D.; McClintock, S. P.; Zakharov, L. N.; Haley, M. M. *Angew. Chem., Int. Ed.* **2011**, *50*, 1127. (b) Shimizu, A.; Tobe, Y. *Angew. Chem., Int. Ed.* **2011**, *50*, 6906. (c) Shimizu, A.; Kishi, R.; Nakano, M.; Shiomi, D.; Sato, K.; Takui, T.; Hisaki, I.; Miyata, M.; Tobe, Y. *Angew. Chem., Int. Ed.* **2013**, *52*, 6076. (d) Miyoshi, H.; Nobusue, S.; Shimizu, A.; Hisaki, I.; Miyatab, M.; Tobe, Y. *Chem. Sci.* **2014**, *5*, 163. (e) Shimizu, A.; Nobusue, S.; Miyoshi, H.; Tobe, Y. *Pure Appl. Chem.* **2014**, *86*, 517.
(11) (a) Konishi, A.; Hirao, Y.; Nakano, M.; Shimizu, A.; Botek, E.; Champagne, B.; Shiomi, D.; Sato, K.; Takui, T.; Matsumoto, K.; Kurata, H.; Kubo, T. *J. Am. Chem. Soc.* **2010**, *132*, 11021. (b) Konishi, A.; Hirao, Y.; Matsumoto, K.; Kurata, H.; Kishi, R.; Shigeta, Y.; Nakano, M.; Tokunaga, K.; Kamada, K.; Kubo, T. *J. Am. Chem. Soc.* **2013**, *135*, 1430. (c) Liu, J.; Ravat, P.; Wagner, M.; Baumgarten, M.; Feng, X.; Müllen, K. *Angew. Chem., Int. Ed.* **2015**, *54*, 12442.
(12) (a) Zhu, X.; Tsuji, H.; Nakabayashi, H.; Ohkoshi, S.; Nakamura, E. *J. Am. Chem. Soc.* **2011**, *133*, 16342. (b) Zeng, Z.; Ishida, M.; Zafra, J. L.; Zhu, X.; Sung, Y. M.; Bao, N.; Webster, R. D.; Lee, B. S.; Li, R.-W.; Zeng, W.; Li, Y.; Chi, C.; López Navarrete, J. T.; Ding, J.; Casado, J.; Kim, D.; Wu, J. *J. Am. Chem. Soc.* **2013**, *135*, 6363. (c) Zeng, Z.; Lee, S.; Zafra, J. L.; Ishida, M.; Zhu, X.; Sun, Z.; Ni, Y.; Webster, R. D.; Li, R.-W.; López Navarrete, J. T.; Chi, C.; Ding, J.; Casado, J.; Kim, D.; Wu, J. *Angew. Chem., Int. Ed.* **2013**, *52*, 8561. (d) Zeng, Z.; Lee, S.; Son, M.; Fukuda, K.; Burrezo, P. M.; Zhu, X.; Qi, Q.; Li, R.-W.; López Navarrete, J. T.; Ding, J.; Casado, J.; Nakano, M.; Kim, D.; Wu, J. *J. Am. Chem. Soc.* **2015**, *137*, 8572.
(13) (a) Nobusue, S.; Miyoshi, H.; Shimizu, A.; Hisaki, I.; Fukuda, K.; Nakano, M.; Tobe, Y. *Angew. Chem., Int. Ed.* **2015**, *54*, 2090. (b) Hu, P.; Lee, S.; Herng, S. T.; Aratani, N.; Goncalves, T. P.; Qi, Q.; Si, X.; Yamada, H.; Huang, K. − W.; Ding, J.; Kim, D.; Wu, J. *J. Am. Chem. Soc.* **2016**, *138*, 1065. (c) Das, S.; Herng, T. S.; Zafra, J. L.; Burrezo, P. M.; Kitano, M.; Ishida, M.; Gopalakrishna, T. Y.; Hu, P.; Osuka, A.; Casado, J.; Ding, J.; Casanova, D.; Wu, J. *J. Am. Chem. Soc.* **2016**, *138*, 7782.
(14) Zeng, Z.; Sung, Y. M.; Bao, N.; Tan, D.; Lee, R.; Zafra, J. L.; Lee, B. S.; Ishida, M.; Ding, J.; López Navarrete, J. T.; Li, Y.; Zeng, W.; Kim, D.; Huang, K.-W.; Webster, R. D.; Casado, J.; Wu, J. *J. Am. Chem. Soc.* **2012**, *134*, 14513.
(15) Tian, Y.; Uchida, K.; Kurata, H.; Hirao, Y.; Nishiuchi, T.; Kubo, T. *J. Am. Chem. Soc.* **2014**, *136*, 12784.
(16) We also tried to synthesize the corresponding polymer by using Suzuki coupling between **4** and its boronic ester under various conditions, but only low molecular weight linear oligomers and macrocycles were obtained. The separation and physical properties of macrocyclic fluorenyl oligomers will be reported in a future publication.
(17) Crystallographic data of **FR-1** and **FR-2** are deposited in the Cambridge Crystallographic Data Center (CCDC) with the CCDC numbers 1482791 and 1483187, respectively.
(18) (a) Becke, A. D. *J. Chem. Phys.* **1993**, *98*, 5648. (b) Lee, C.; Yang, W.; Parr, R. G. *Phys. Rev. B: Condens. Matter Mater. Phys.* **1988**, *37*, 785. (c) Yanai, T.; Tew, D.; Handy, N. *Chem. Phys. Lett.* **2004**, *393*, 51.
(19) Minami, T.; Nakano, M. *J. Phys. Chem. Lett.* **2012**, *3*, 145.
(20) Casanova, D.; Head-Gordon, M. *Phys. Chem. Chem. Phys.* **2009**, *11*, 9779.
(21) Head-Gordon, M. *Chem. Phys. Lett.* **2003**, *372*, 508.
(22) (a) Bleaney, B.; Bowers, K. D. *Proc. R. Soc. London, Ser. A* **1952**, *214*, 451. (b) Kahn, O. *Molecular Magnetis*; VCH: New York, 1993.
(23) (a) Teki, Y.; Miyamoto, S.; Nakatsuji, M.; Miura, Y. *J. Am. Chem. Soc.* **2001**, *123*, 294. (b) Yamamoto, Y.; Wakamatsu, K.; Iwanaga, T.; Sato, H.; Toyota, S. *Chem. - Asian J.* **2016**, *11*, 1370.
(24) (a) Nakano, M.; Nagao, H.; Yamaguchi, K. *Phys. Rev. A: At., Mol., Opt. Phys.* **1997**, *55*, 1503. (b) Nakano, M.; Kishi, R.; Nitta, T.; Kubo, T.; Nakasuji, K.; Kamada, K.; Ohta, K.; Champagne, B.; Botek, E.; Yamaguchi, K. *J. Phys. Chem. A* **2005**, *109*, 885. (c) Nakano, M.; Kubo, T.; Kamada, K.; Ohta, K.; Kishi, R.; Ohta, S.; Nakagawa, N.; Takahashi, H.; Furukawa, S.; Morita, Y.; Nakasuji, K.; Yamaguchi, K. *Chem. Phys. Lett.* **2006**, *418*, 142. (d) Ohta, S.; Nakano, M.; Kubo, K.; Kamada, K.; Ohta, K.; Kishi, R.; Nakagawa, N.; Champagne, B.; Botek, E.; Takebe, A.; Umezaki, S.; Nate, M.; Takahashi, H.; Furukawa, S.; Morita, Y.; Nakasuji, K.; Yamaguchi, K. *J. Phys. Chem. A* **2007**, *111*, 3633. (e) Nakano, M.; Kishi, R.; Takebe, A.; Nate, M.; Takahashi, H.; Kubo, T.; Kamada, K.; Ohta, K.; Champagne, B.; Botek, E. *Comput. Lett.* **2007**, *3*, 333. (f) Kamada, K.; Ohta, K.; Kubo, T.; Shimizu, A.; Morita, Y.; Nakasuji, K.; Kishi, R.; Ohta, S.; Furukawa, S. I.; Takahashi, H.; Nakano, M. *Angew. Chem., Int. Ed.* **2007**, *46*, 3544. (g) Nakano, M.; Kishi, R.; Ohta, S.; Takahashi, H.; Kubo, T.; Kamada, K.; Ohta, K.; Botek, E.; Champagne, B. *Phys. Rev. Lett.* **2007**, *99*, 033001.
(25) (a) Brédas, J. L.; Silbey, R.; Boudreaux, D. S.; Chance, R. R. *J. Am. Chem. Soc.* **1983**, *105*, 6555. (b) Chen, P.; Marshall, A. S.; Chi, S.-H.; Yin, X.; Perry, J. W.; Jäkle, F. *Chem. - Eur. J.* **2015**, *21*, 18237.

DOI: 10.1021/jacs.6b08138
J. Am. Chem. Soc. 2016, 138, 13048−13058